

Performance Analysis of Hierarchically Combined Practical Beamforming Methods

Beneyam B. Haile¹ · Jyri Hämäläinen¹

Published online: 5 April 2015

© The Author(s) 2015. This article is published with open access at Springerlink.com

Abstract In literature various limited-feedback beamforming methods applied in co-located and distributed antenna systems have been proposed for enhancing wireless link spectral efficiency and reliability. We focus on practical limited-feedback methods and introduce a hierarchical feedback structure, whereby co-located/distributed transmit antennas are organized into two or more groups. To facilitate robust and flexible use of channel state information we apply independent feedback to antenna groups and between the groups. This structure provides additional implementation flexibility under practical constraints, particularly for coordinated multipoint (CoMP) systems. For the presented methods with hierarchical control structure, we compute closed-form expressions for the signal-to-noise power ratio gain, the fading figure and the average bit-error-probability. Although hierarchical structure leads in some cases to suboptimal methods, results show that performance loss against upper bound given by transmitter equal gain combining is negligible even when number of feedback bits is small. Thus, it is concluded that the hierarchical feedback that is robust against errors can be effectively used when antennas form natural groups like in e.g. CoMP transmission.

Keywords Hierarchical beamforming · Transmit beamforming · Coordinated multipoint (CoMP) · Multiple-input multiple-output (MIMO)

1 Introduction

In recent years, various limited-feedback beamforming methods have been proposed and studied in order to improve the robustness and data rate of wireless link [1–7]. Some of these methods have been adopted to practical systems, for instance, into the 3rd generation

✉ Beneyam B. Haile
beneyam.haile@aalto.fi

¹ Department of Communications and Networking, Aalto University, P.O. Box 13000, 00076 Espoo, Finland

partnership project (3GPP) high speed packet access (HSPA) and long term evolution (LTE) systems, to be used in either co-located or distributed transmission modes. In the co-located scenario, closely-spaced antennas transmit the same information exploiting channel state information (CSI) to maximize the received signal-to-noise ratio (SNR) [8–12]. For the distributed beamforming scenario techniques such as coordinated multipoint (CoMP) joint transmission (JT) have been introduced and incorporated into the practical systems mainly to improve link reliability and data rate of cell-edge users [13–17].

The performance differences between beamforming methods may depend on the proposed limited feedback method, backhaul quality (especially in case of inter-site CoMP) and other implementation factors. Let us briefly recall some previous works on these aspects:

1. *Feedback* There is a trade-off between amount of CSI available at the transmitter side and link performance improvement. In general, the more there is feedback capacity, the better the link performance, see e.g. [4, 5, 12, 17–19]. The performance degradation due to feedback errors is presented in [20] while [21] shows that it is possible to design efficient codebooks even under imperfect feedback system. Furthermore, mechanisms to mitigate negative impact of feedback errors and delay are proposed in [22] while achievable rate analysis for JT CoMP under imperfect feedback is presented in [23, 24].
2. *Backhaul* To reach the expected performance, inter-site JT CoMP methods set strict backhaul capacity and latency requirements [15]. We note that the CoMP methods studied and incorporated in 3GPP release 11 assume ideal backhaul with infinite capacity and zero latency [13]. The 3GPP methods may work with high-capacity and low latency wireline backhaul (e.g. fiber). However, the capacity and latency requirements need to be relaxed while using less ideal backhaul technologies. As a result various CoMP methods under non-ideal backhaul has been recently studied [25, 26]. While [26] presents two algorithms that can significantly reduce backhaul capacity requirements, [25] focus on 3GPP release 12 CoMP assuming non-ideal backhaul.

We introduce in this paper a hierarchical beamforming structure whereby combination of beamforming methods can be applied using either co-located or distributed antenna systems. The applied hierarchical structure is depicted in Fig. 1 where transmit antennas (co-located or distributed) are organized into M groups. The groups are organized in such a

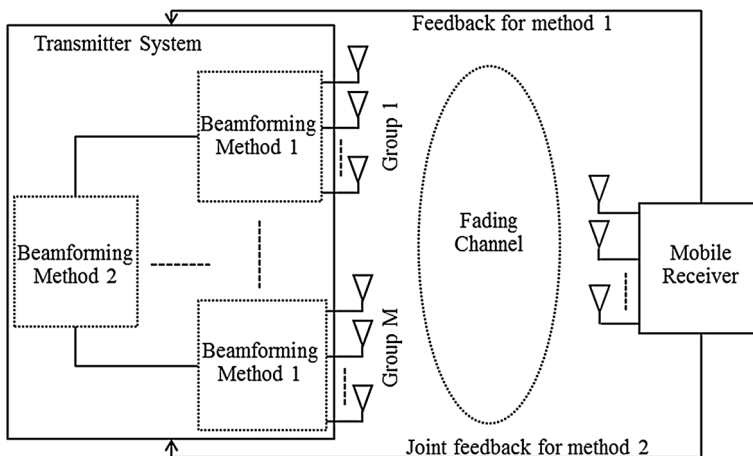


Fig. 1 Illustration of the beamforming system

way that appropriate beamforming method is applied within each group (shown in Fig. 1 as Method 1) as well as between the groups (shown in Fig. 1 as Method 2). The receiver sends to each group signalling information needed in methods 1 and joint signalling information applied in method 2. The joint feedback is based on the resultant signals from all groups after precoding. With this hierarchical structure, we attain the freedom to combine different beamforming methods. Furthermore, in CoMP JT the feedback signalling towards each base station can be carried out through separate feedback channels.

In what follow, we also mathematically analyze the performance of the proposed hierarchical system when combining two practical beamforming methods: the so-called quantized co-phasing (QCP) which is applied in HSPA and LTE, and transmit selection combining (TSC). We note that these methods have different performance and feedback requirements [20]. We derive closed-form expressions for the expected SNR, fading figure and average bit error probability (BEP) when assuming different combinations of QCP and TSC methods. While exact expressions for the expected SNR and the fading figure are obtained, we deduce tight approximations for the average BEP using distributions based on calculated exact moment expressions. While the SNR gain provides insight on the benefit obtained from the coherent combining, results on the fading figure and the average BEP demonstrate the amount of achieved diversity gain.

The rest of the paper is structured as follows. Section 2 presents the system model and the limited feedback precoding methods. Section 3 recalls definitions of the applied performance metrics and respective expressions for the reference methods. In Sects. 4–6, we analyse the hierarchical methods and present the mathematical formulations for the SNR gain, the fading figure and the average BEP. Analytical results are validated in Sect. 7 and discussion on the results is carried out. Finally, Sect. 8 concludes the paper highlighting the core contributions.

2 System Model

2.1 Signal Model and Assumptions

Figure 2 illustrates the structure of transmission system with 2×2 antennas. The model can be easily generalized to larger group and number of antennas, but for simplicity we have focused on the case of 2×2 antennas. We have assumed flexible feedback structure where antenna pairs can be either on separate base station sites or co-located on the same

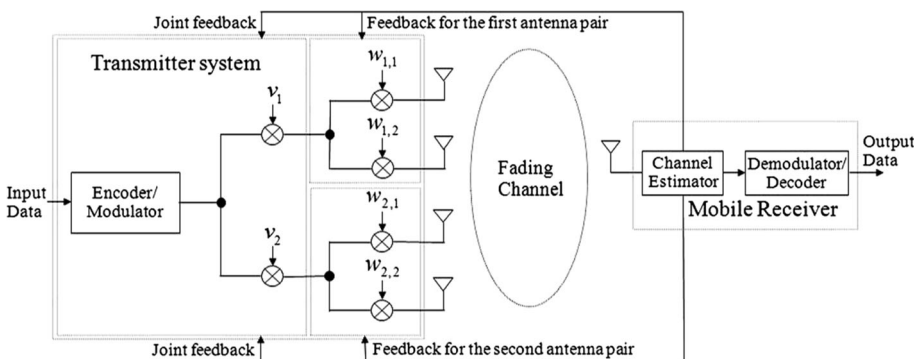


Fig. 2 Transmission and feedback system that is composed by pairs of antennas

site. In former case mobile receiver use two separate control channels to send precoding feedback. Thus, precoding information for the first base station indicates the preferred transmit beamforming vector $\mathbf{w}_1 = (w_{1,1}, w_{1,2})$ and weight v_1 that is used to adjust the sum signal from first pair of antennas against the sum signal from the second pair of antennas. Similarly precoding information is provided for the second base station to select beamforming vector $\mathbf{w}_2 = (w_{2,1}, w_{2,2})$ and weight v_2 . If all antennas are co-located on the same base station site, then the same precoding information is sent through single control channel towards serving base station. We note that the introduced hierarchical feedback structure is flexible so that it can be used for both cooperative multipoint transmission from separate two-antenna base stations and for four-antenna transmission from a single base station.

Now, the received signal in the mobile station is of the form:

$$\begin{aligned} r &= ((\mathbf{h}_1 \cdot \mathbf{w}_1)v_1 + (\mathbf{h}_2 \cdot \mathbf{w}_2)v_2)s + n \\ &= H(\mathbf{w}, \mathbf{v})s + n. \end{aligned} \quad (1)$$

Here s is the transmitted symbol, $\mathbf{h}_k = (h_{k,1}, h_{k,2})$, $k = 1, 2$ represent the complex channel gains, n refers to zero-mean complex Gaussian noise, vectors \mathbf{w}_k , $k = 1, 2$ refer to the complex transmit weights on different antenna pairs such that $\|\mathbf{w}_k\| = 1$, and $\mathbf{v} = (v_1, v_2)$ is the normalized ($\|\mathbf{v}\| = 1$) complex transmit weight vector applied to adjust signals from different antenna pairs. The weight vector \mathbf{v} is selected based on a precoding method applied between pairs while \mathbf{w}_k is selected based on a method applied within the k th antenna pair. We will present the methods studied in this work in the next Subsection. Given the received signal (1) and quantization for the transmit weights, the weights that maximize SNR in the reception can be found after evaluating received signal strength $|r|$ for all possible weight vectors.

We make the following assumptions:

- (A1) There are two antenna pairs at the transmitter and a single-element antenna at the receiver.
- (A2) A block and flat fading channel model is considered. Thus, channel gains remain constant during each frame of transmitted symbols, and channel responses from temporally separate transmission frames are independent. Furthermore, the channel coefficients $h_{k,l} = \sqrt{\gamma_{k,l}} e^{j\phi_{k,l}}$ ($k, l = 1, 2$) are *independent and identically distributed* (i.i.d.) zero-mean complex Gaussian random variables. Then component channel powers $\gamma_{k,l}$ follow exponential distribution and phases $\phi_{k,l}$ are uniformly distributed.
- (A3) Channel coefficients are perfectly known at the receiver side.
- (A4) Selection of transmit weights \mathbf{w}_k , $k = 1, 2$ and \mathbf{v} is based on *short-term* channel state feedback that is available at the transmitter side without errors or latency.

Let us briefly discuss on the justification of the assumptions. In (A1) we could assume multi-antenna reception like maximum ratio combining or receiver antenna selection instead of single antenna reception. This would lead to technically more complex analysis but the principles of the analytical treatment of the problem would remain the same. Therefore we have restricted analysis into the single antenna receiver case.

In mobile systems the co-located four-antenna systems are usually implemented by applying spatially separated pairs of cross-polarized antennas [27]. In such deployment the separation distance between antenna pairs is several carrier wavelengths and as a result correlation between antenna pairs is small especially in urban environments, see e.g. [28]. On the other hand, in case of cooperative multipoint transmission from separate two-

antenna base stations the mutual distance between antenna pairs is large and there is no correlation between pairs. The correlation between antennas within the co-located pairs depends on the antenna construction. It is known that correlation can be kept small in urban areas using cross-polarized antenna branches, see e.g. [27, 29–31]. Since cross-polarized antennas can be co-located in the same antenna box the resulting compact antenna design has been popular in practical applications. Based on these observations we have ignored the antenna correlation. Yet, we note that in rural area deployment correlation may have impact to the system performance and thus, our analysis is mostly valid on urban area where line-of-sight very rarely occurs between base station and mobile receiver.

Due to assumption (A3) we presume perfect channel estimation. This is a conventional assumption when focus is on performance of multi-antenna processing method. The assumption (A4) is widely used as well and we discuss on the feedback methods in more details in the following section. Yet, it is good to acknowledge that for a good performance the mobile receiver needs only send few bit feedback words that refer to precoding vectors \mathbf{w}_m , $m = 1, 2$ and \mathbf{v} according to applied codebook. Due to receiver mobility the feedback protocol should be executed well within the channel coherence time that depends on the receiver speed and carrier wavelength. In e.g. HSPA and LTE systems the feedback is provided within few milliseconds and precoding will work well up to speeds of tens of kilometers per hour. In practise the impact of latency is very small and can be ignored in urban low-mobility environments (indoor and outdoor pedestrians).

2.2 Precoding Methods

We have adopted a hierarchical feedback structure with two levels of feedback. Namely, the feedback to different pairs of antennas and the feedback for adjusting sum signals from antenna pairs are separate. This provides some benefits especially in case of cooperative multipoint transmission:

- If antenna pairs are located to different base station sites, then mobile terminal can easily provide antenna pair specific feedback over two separate control channels. In signal model this feedback refers to \mathbf{w}_1 and \mathbf{w}_2 .
- If cooperative transmission is applied, then joint feedback only consists of index referring to a single feedback weight. In signal model the corresponding weights are v_1 for the first base station site and v_2 for the second base station site.
- Different kind of precoding methods can be used within antenna pairs and over the pairs.

The last of the above advantages can have practical value when, for example, antenna configurations are different in base stations that cooperate in transmission. Furthermore, if mean signal strength from either of the base stations is stronger, then more accurate feedback can be provided for it in adaptive feedback system.

In the following we introduce simple feedback (precoding) methods that are obtained as combinations of antenna selection and QCP. These methods are suboptimal in nature but they admit practical value since e.g. QCP is applied in HSPA and LTE and antenna selection provides a natural reference for comparisons. Moreover, feedback overhead can be kept very small when using these methods.

Let us first introduce a general two-branch precoding method. Assume that \mathbf{g} is two-dimensional complex channel vector and \mathbf{u} is the applied precoding weight vector. Then power of the composed channel $H = \mathbf{g} \cdot \mathbf{u}$ is maximized after solving

$$\text{Find } \hat{\mathbf{u}} \in \mathbf{W} : \quad |\mathbf{g} \cdot \hat{\mathbf{u}}| = \max\{|\mathbf{g} \cdot \mathbf{u}| : \mathbf{u} \in \mathbf{W}\}. \quad (2)$$

In case of antenna selection $\mathbf{W} = \{(1, 0), (0, 1)\}$ and in case of quantized co-phasing \mathbf{W} consists of vectors $(1, e^{j\phi_n})/\sqrt{2}$, where $\phi_n = 2(n-1)\pi/2^N$, $n \in \{1, 2, \dots, 2^N\}$ and N is the number of phase feedback bits.

When the proposed hierarchical feedback structure is used we define \mathbf{w}_1 and \mathbf{w}_2 for different antenna pairs according to (2) and set $g_1 = \mathbf{h}_1 \cdot \mathbf{w}_1$, $g_2 = \mathbf{h}_2 \cdot \mathbf{w}_2$ and define \mathbf{v} using again (2). In this way we obtain four method combinations:

1. *Selection-Selection (SS)* In this method combination, selection scheme is applied both within antenna pairs and between antenna pairs. In other way, it means using the antenna with the best channel power which is the same as the traditional and well-studied selection technique. We need here a total of two feedback bits: one to select an antenna pair and the other to select an antenna from the selected antenna pair.
2. *Selection-Quantized Co-phasing (SC)* In here, QCP is applied in each pair and selection is applied between pairs. Thus, we select an antenna pair that provides better SNR after QCP. As a result, the method combination needs a total of $N + 1$ number of feedback bits to be operational, N bits for QCP applied in the selected antenna pair and 1 bit for the selection.
3. *Quantized Co-phasing-Selection (CS)* In this combination, selection is made in each antenna pair and QCP is applied between resultants of the selections. Mobile receiver needs to send a total of $N + 2$ feedback bits to make CS operational: N bits for the QCP and 2 bits for the selections.
4. *Quantized Co-phasing - Quantized Co-phasing (CC)* In this case, we define \mathbf{w}_1 , \mathbf{w}_2 and \mathbf{v} based on QCP scheme. Then the method requires a total of $N_1 + N_2 + N_3$ feedback bits where N_1 and N_2 denote number of bits used for the QCPs applied in the first and second antenna pairs and N_3 denotes number of bits used for the QCP between the pairs. The QCPs that are applied independently in the pairs and between the pairs can be considered as different technique as they can use different number of feedback bits. Furthermore, CC resembles equal gain transmission when large phase feedback information is available at the transmitter (i.e. $N_1 \gg 1$, $N_2 \gg 1$, and $N_3 \gg 1$). We denote this case as CC with Large feedback bits (CCL).

In the following analysis, we treat SS as a reference method since its analysis is same with well-studied transmit selection technique. For comparison purpose, we also recall results when full CSI is available at transmitter side. We refer this case hereafter as Full Information (FI) method.

3 Performance Metrics and Reference Methods

The received SNR after a given hierarchical precoding method is of the form

$$Z = |H(\hat{\mathbf{w}}, \hat{\mathbf{v}})|^2, \quad (3)$$

where $\hat{\mathbf{w}}$ and $\hat{\mathbf{v}}$ are selected using (2). Then coherent combining gain is denoted by \mathcal{G} and fading figure is denoted by \mathcal{F} and they are defined as

$$\mathcal{G} = \mathbb{E}[Z], \quad \mathcal{F} = \frac{\mathcal{G}^2}{\mathbb{E}[Z^2] - \mathcal{G}^2}. \quad (4)$$

The former provides insight on the beamforming gain and hereafter we refer it as SNR gain. The latter is a function of the first and second moments and it describes the diversity benefit from applied method showing degree of SNR variation [32]. More insight on performance benefits can be obtained from average BEP which is expressed as

$$\bar{P} = \int_0^{\infty} P_{mod}(\bar{\gamma}z) f_Z(z) dz, \quad (5)$$

where $\bar{\gamma}$ is the transmit SNR or the ratio between symbol energy and noise spectral density, and $P_{mod}(\cdot)$ is the error rate of a modulation in terms of SNR. We present in this work analysis for BPSK modulation where

$$P_{mod}(\bar{\gamma}r) = Q\left(\sqrt{2\bar{\gamma}r}\right). \quad (6)$$

Let us now recall closed-form expressions for the performance metrics when reference methods are applied for transmission.

For SS method combination, we find from (3) that

$$Z_{ss} = \max\{\gamma_{1,1}, \gamma_{1,2}, \gamma_{2,1}, \gamma_{2,2}\}.$$

Expressions for PDF is well-known such that $f_{Z_{ss}}(z) = Me^{-z}(1 - e^{-z})^{M-1}$ where M denotes number of available antennas. The n th moment is given by [33]

$$E[Z_{ss}^n] = \sum_{i=1}^M \binom{M}{i} \frac{(-1)^{i+1} n!}{i^n}, \quad (7)$$

and we also recall that an average BEP expression is of the form [33]

$$\bar{P}_{ss} = \frac{1}{2} \sum_{i=0}^M (-1)^i \binom{M}{i} \sqrt{\frac{1}{1+i}}. \quad (8)$$

While SS gives performance lower bound, the upper bound for the performance is obtained when full CSI is available at transmitter. Then instantaneous SNR Z_{fi} follows chi-square distribution with $2M$ degrees of freedom: $f_{Z_{fi}}(z) = 1/\Gamma(M)z^{M-1}e^{-z}$. Corresponding n th moment and average BEP expressions are formulated as [33]

$$E[Z_{ss}^n] = \frac{\Gamma(M+n)}{\Gamma(M)} \quad (9)$$

and

$$\bar{P}_{fi} = \left(\frac{\sqrt{2}-1}{2\sqrt{2}}\right)^{M-1} \sum_{i=0}^{M-1} \binom{M-1+i}{i} \left(\frac{\sqrt{2}+1}{2\sqrt{2}}\right)^i. \quad (10)$$

For both SS and FI methods, we can find expressions for both \mathcal{G} and \mathcal{F} using first and second moment expressions of (7) and (9) with $M = 4$.

4 SC Method

If QCP is used within antenna pairs and selection is used between antenna pairs, then the SNR becomes

$$Z_{sc} = \frac{1}{2} \max\{\gamma_{1,1} + \gamma_{1,2} + 2\sqrt{\gamma_{1,1}\gamma_{1,2}} \cos \theta_1, \gamma_{2,1} + \gamma_{2,2} + 2\sqrt{\gamma_{2,1}\gamma_{2,2}} \cos \theta_2\}, \tag{11}$$

where $\theta_k = \phi_{k,2} - \phi_{k,1} + \phi_k$. Hence $\phi_k = 2(n_k - 1)\pi/2^{N_k}$ refers the selected phase for the QCP method applied in the k th antenna pair with N_k feedback bits. Note here that the variable θ_k follows uniform distribution on the range $(-\pi/2^{N_k}, \pi/2^{N_k})$ and SNR's $\gamma_{k,l}$ are independent and identically distributed exponential variables according to (A2). The impact of quantized co-phasing on resultant SNR of k th antenna pair is further illustrated using phasor diagram in Fig. 3. We note that X and X' denote SNRs with and without co-phasing, respectively, for the 1st antenna pair. Similarly, Y and Y' denote SNRs with and without co-phasing for the 2nd antenna pair.

In order to present an accurate approximation for distribution of Z_{sc} , we approximate distributions of X and Y using error corrected chi-square distribution with 4 degrees of freedom (see Appendix 1). Accordingly, we set

$$f_X(x) = m_x^2 e^{-m_x x} \sum_{i=1}^3 a_i^x x^i \quad f_Y(y) = m_y^2 e^{-m_y y} \sum_{i=1}^3 a_i^y y^i, \tag{12}$$

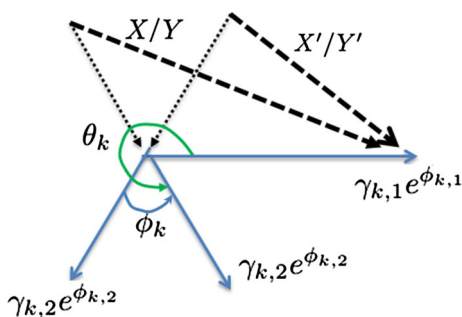
where $m_p = 2/E[P]$, $a_3^p = \frac{4E[P^2]}{3E[P]^4} - \frac{2}{E[P]^2}$, $a_2^p = -3E[P]a_3^p$, and $a_1^p = -\frac{E[P]}{2}a_2 + 1$. Straight-forward moment computations provide

$$\begin{aligned} E[X] &= 2 + \frac{\pi \operatorname{sinc}(\pi/2^{N_1})}{2}, & E[Y] &= 2 + \frac{\pi \operatorname{sinc}(\pi/2^{N_2})}{2}, \\ E[X^2] &= 8 + 2 \operatorname{sinc}(\pi/2^{N_1-1}) + 3\pi \operatorname{sinc}(\pi/2^{N_1}), \\ E[Y^2] &= 8 + 2 \operatorname{sinc}(\pi/2^{N_2-1}) + 3\pi \operatorname{sinc}(\pi/2^{N_2}). \end{aligned} \tag{13}$$

We then compute PDF for Z_{sc} using known expression for distribution of maximum over two independent random variables given in [34] and approximations in (12) to obtain

$$\begin{aligned} f_{Z_{sc}}(z) &= \sum_{i=1}^3 \sum_{j=1}^3 \left(\frac{A_{ij}^{xy} z^i}{e^{2m_x z}} - \sum_{k=0}^j \frac{B_{ij}^{xy}(2z)^{i+k}}{k! m_y^{j-k+1} e^{2(m_x+m_y)z}} \right) \\ &+ \sum_{i=1}^3 \sum_{j=1}^3 \left(\frac{A_{ij}^{yx} z^i}{e^{2m_y z}} - \sum_{k=0}^j \frac{B_{ij}^{yx}(2z)^{i+k}}{k! m_x^{j-k+1} e^{2(m_x+m_y)z}} \right), \end{aligned} \tag{14}$$

Fig. 3 Phasor representation of co-phasing in the k th antenna pair



where

$$A_{ij}^{xy} = \frac{2^{i+1} m_x^2 a_i^x a_j^y!}{m_y^{j-1}} \quad B_{ij}^{xy} = 2m_x^2 m_y^2 a_i^x a_j^y!. \tag{15}$$

We note that if $N_1 = N_2$, then $m_x = m_y$, $A_{ij}^{xy} = A_{ij}^{yx}$, $B_{ij}^{xy} = B_{ij}^{yx}$ and the PDF of Z_{sc} reduces to a simple form

$$f_{Z_{sc}}(z) = 2 \sum_{i=1}^3 \sum_{j=1}^3 \frac{A_{ij}^{xy} z^i}{e^{2m_x z}} - \sum_{k=0}^j \frac{B_{ij}^{xy} (2z)^{i+k}}{k! m_x^{j-k+1} e^{4m_x z}}. \tag{16}$$

The n th moment for Z_{sc} we derive by substituting (6) in the integral $\int_0^\infty z^n f(z) dz$ and using definite integral form given in [35, 3.35 (3)]. The resulting moment expression is given by

$$\begin{aligned} E[Z_{sc}^n] &= \sum_{i=1}^3 \sum_{j=1}^3 \frac{A_{ij}^{xy} (i+n)!}{(2m_x)^{i+n+1}} - B_{ij}^{xy} \sum_{k=0}^j \frac{2^{-n} (i+k+n)! m_y^{k-j-1}}{2k! (m_x + m_y)^{i+k+n+1}} \\ &+ \sum_{i=1}^3 \sum_{j=1}^3 \frac{A_{ij}^{yx} (i+n)!}{(2m_y)^{i+n+1}} - B_{ij}^{yx} \sum_{k=0}^j \frac{2^{-n} (i+k+n)! m_x^{k-j-1}}{2k! (m_x + m_y)^{i+k+n+1}}. \end{aligned} \tag{17}$$

If $N_1 = N_2$, then we have

$$E[Z_{sc}^n] = 2 \sum_{i=1}^3 \sum_{j=1}^3 \left(\frac{A_{ij}^{xy} (i+n)!}{(2m_x)^{i+n+1}} - B_{ij}^{xy} \sum_{k=0}^j \frac{(i+k+n)! m_x^{k-j-1}}{2^{n+1} k! (2m_x)^{i+k+n+1}} \right). \tag{18}$$

Expressions for \mathcal{G}_{sc} and \mathcal{F}_{sc} are obtained using (4) and expressions of first and second moments of (17) and (18).

We compute the BEP integral in (5) by substituting distribution in (14) and equation (6). After rearranging resulting integrals and compute them, we obtain

$$\begin{aligned} \bar{P}_{sc} &= \sum_{i=1}^3 \sum_{j=1}^3 \left(A_{ij}^{xy} J_{i+1}(2m_x, 2\bar{\gamma}) - B_{ij}^{xy} \sum_{k=0}^j \frac{2^{i+k} J_{i+k+1}(2(m_x + m_y), 2\bar{\gamma})}{k! m_y^{j-k+1}} \right) \\ &+ \sum_{i=1}^3 \sum_{j=1}^3 \left(A_{ij}^{yx} J_{i+1}(2m_y, 2\bar{\gamma}) - B_{ij}^{yx} \sum_{k=0}^j \frac{2^{i+k} J_{i+k+1}(2(m_x + m_y), 2\bar{\gamma})}{k! m_x^{j-k+1}} \right), \end{aligned} \tag{19}$$

where

$$J_s(a, b) = \int_0^\infty t^{s-1} e^{-at} Q(\sqrt{bt}) dt. \tag{20}$$

The function $J_s(a, b)$ in (20) admits closed-form expression which is presented in Appendix 5A of [36]:

$$J_s(a, b) = \frac{\Gamma(s)}{2a^s} \left[1 - \sqrt{\frac{b}{b+2a}} \sum_{k=0}^{s-1} \binom{2k}{k} \left(\frac{a}{4a+2b} \right)^k \right]. \tag{21}$$

When N_1 is equal to N_2 , the average BEP expression attains a simpler form

$$\bar{P}_{sc} = 2 \sum_{i=1}^3 \sum_{j=1}^3 \left(A_{ij}^{xy} J_{i+1}(2m_x, 2\bar{\gamma}) - B_{ij}^{xy} \sum_{k=0}^j \frac{2^{i+k} J_{i+k+1}(4m_x, 2\bar{\gamma})}{k! m_y^{j-k+1}} \right). \tag{22}$$

5 CS Method

In CS method combination, selection is applied within antenna pairs and QCP is applied between the pairs. As a result, the instantaneous SNR attain the form

$$Z_{cs} = \frac{1}{2} (\gamma_1 + \gamma_2 + 2\sqrt{\gamma_1\gamma_2} \cos \theta_3), \tag{23}$$

where $\gamma_1 = \max\{\gamma_{1,1}, \gamma_{1,2}\}$, $\gamma_2 = \max\{\gamma_{2,1}, \gamma_{2,2}\}$, and $\theta_3 = \psi_2 - \psi_1 + \phi_3 \sim U(-\pi/2^{N_3}, \pi/2^{N_3})$. Note that ψ_i denotes phase of channel with maximum power and $\phi_3 = 2(n_3 - 1)\pi/2^{N_3}$ denotes selected phase for QCP when using N_3 phase bits, according to (2). Impact of the co-phasing between antenna pairs on the resultant SNR is further illustrated using phasor diagram in Fig. 4. The parameter Z'_{cs} denotes resultant SNR in the absence of co-phasing.

In order to compute the first and second moments of Z_{cs} , we first need to know expected value expressions for $\cos \theta_3$, $\cos^2 \theta_3$, and γ_i^j , $i \in \{1, 2\}$, $j \in \{1/2, 3/2, 1, 2\}$. Applying elementary integration, we find that

$$\begin{aligned} E[\cos \theta_3] &= \text{sinc}(\pi/2^{N_3}), & E[\cos^2 \theta_3] &= (1 + \text{sinc}(\pi/2^{N_3-1}))/2, \\ E[\gamma_i^j] &= 2(1 - 2^{-j-1})\Gamma(j + 1), \end{aligned} \tag{24}$$

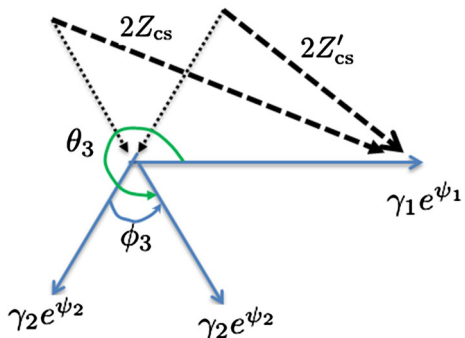
where $\text{sinc}(x) = \sin(x)/x$ and $\Gamma(\cdot)$ refers to Gamma function. We can now use these expressions when composing first and second moments of Z_{cs} in (23). As a result, we obtain

$$G_{cs} = \frac{3}{2} + \frac{(2\sqrt{2} - 1)^2}{8} \pi \text{sinc}(\pi/2^{N_3}), \tag{25}$$

and

$$E[Z_{cs}^2] = \frac{7}{4} + \frac{9}{8} (2 + \text{sinc}(\pi/2^{N_3-1})) + \frac{3(17 - 6\sqrt{2})}{16} \pi \text{sinc}(\pi/2^{N_3}). \tag{26}$$

Fig. 4 Phasor representation of co-phasing between antenna pair



Then expression for \mathcal{F}_{cs} is obtained using (4), (25) and (26).

We approximate PDF of Z_{cs} based on the exactly computed first and second moments given in (25) and (26). We use the error corrected chi-square distribution with 8 degrees of freedom (see Appendix, equation (38)) to find a PDF approximation of the form

$$f_{Z_{cs}}(z) = \frac{128}{3\mathcal{G}_{cs}^4} e^{-\frac{4}{\mathcal{G}_{cs}}z} \sum_{i=1}^3 a_i z^{i+2}, \tag{27}$$

where

$$a_3 = \frac{32 E[Z_{cs}^2]}{5 \mathcal{G}_{cs}^4} - \frac{8}{\mathcal{G}_{cs}^2}, \quad a_2 = -\frac{5}{2} \mathcal{G}_{cs} a_3^c, \quad a_1 = -\frac{\mathcal{G}_{cs}}{2} a_2 + 1. \tag{28}$$

To find an average BEP expression, we substitute expressions in (27) and (6) into the integral given in (5). Then we express the resulting integral using specific forms $J_s(\cdot, \cdot)$ presented in (20). The resulting average BEP expression is of a form

$$\bar{P}_{cs} = \frac{128}{3\mathcal{G}_{cs}^4} \left[a_3 J_6\left(\frac{4}{\mathcal{G}_{cs}}, 2\bar{\gamma}\right) + a_2 J_5\left(\frac{4}{\mathcal{G}_{cs}}, 2\bar{\gamma}\right) + a_1 J_4\left(\frac{4}{\mathcal{G}_{cs}}, 2\bar{\gamma}\right) \right]. \tag{29}$$

Note that parameters a_3, a_2 and a_1 are defined through (28).

6 CC Method

In this approach, QCP is applied both within and between the antenna pairs and the SNR can be expressed as

$$Z_{cc} = \frac{1}{4} \left(|z_1|^2 + |z_2|^2 + 2|z_1||z_2| \cos \theta_3 \right), \tag{30}$$

where $z_k = \sqrt{\gamma_{k,1}} e^{j\phi_{k,1}} + \sqrt{\gamma_{k,2}} e^{j(\phi_{k,2} + \phi_k)}$. We note that z_k is the resultant signal after QCP is applied at the k th antenna pair using N_k feedback bits. The mutual phase between pairs of signals is given by $\theta_3 = \angle z_2 - \angle z_1 + \phi_3$, where θ_3 is uniformly distributed on the range $(-\pi/2^{N_3}, \pi/2^{N_3})$ and N_3 refers to the number of phase bits when QCP is applied between antenna pairs.

Since $|z_1|, |z_2|$ and θ_3 in (30) are independent, we write the first and second moments as

$$\mathcal{G}_{cc} = \frac{1}{4} \left[E[|z_1|^2] + E[|z_2|^2] + 2E[|z_1|]E[|z_2|] \text{sinc}(\pi/2^{N_3}) \right], \tag{31}$$

and

$$E[Z_{cc}^2] = \frac{1}{16} \left[E[|z_1|^4] + E[|z_2|^4] + 4E[|z_1|^3]E[|z_2|] \text{sinc}(\pi/2^{N_3}) \right. \\ \left. + 4E[|z_1|]E[|z_2|^3] \text{sinc}(\pi/2^{N_3}) + 2E[|z_1|^2]E[|z_2|^2] (2 + \text{sinc}(\pi/2^{N_3-1})) \right]. \tag{32}$$

Note that (31) and (32) are functions of moments of $|z_1|$ and $|z_2|$. The second and fourth moments are straightforward to compute and we find that

$$\begin{aligned} E[|z_i|^2] &= 2 + \frac{\pi \operatorname{sinc}(\pi/2^{N_i})}{2}, \\ E[|z_i|^4] &= 8 + 3\pi \operatorname{sinc}(\pi/2^{N_i}) + 2\operatorname{sinc}(\pi/2^{N_i-1}). \end{aligned} \tag{33}$$

The first and third moments needed for (31) and (32) are obtained from expression for odd moments which is computed in Appendix 2. Then expression for \mathcal{G}_{cc} and \mathcal{F}_{cc} are formulated using (4), (31), (32), (33) and (45).

Similar to the CS method, we approximate the distribution of Z_{cc} using the error corrected chi-square distribution with 8 degrees of freedom. Thus, we can apply (27) after changing the subscript cs by cc in (27). As $f_{Z_{cc}}(z)$ attains the same form with $f_{Z_{cs}}(z)$, we follow same steps used for CS to compute average BEP expression. The result also has the same form as given in (29) except we are using moments computed for CC method.

We note that if N_1, N_2 , and N_3 are large, then SNR in (30) attains the form

$$Z_{ccl} = \frac{1}{4} \left(|z_1|^2 + |z_2|^2 + 2|z_1||z_2| \right) \tag{34}$$

where $z_k = (\sqrt{\gamma_{k,1}} + \sqrt{\gamma_{k,2}})e^{j\phi_k}$. This case is referred to the ideal phase feedback and equivalent with classical equal gain transmission. Straightforward computations show that in this case

$$\mathcal{G}_{ccl} = \frac{4 + 3\pi}{4}, \quad E[Z_{ccl}^2] = \frac{3\pi^2 + 108\pi + 88}{32}. \tag{35}$$

Again, average BEP can be computed in same way as for CC method and result is given by (29) when using moments in (35).

7 Observation and Performance Experiments

Illustrations for SNR gain and fading figure as a function of number of feedback bits are depicted in Figs. 5 and 6, respectively. Solid curves connect analytical results whereas markers refer to numerical results. For comparison, we also present simulation results for non-hierarchical quantized Optimal Joint Co-phasing (OJC) where instantaneous SNR

$$\begin{aligned} Z_{ojc} &= \frac{1}{4} \max\{|h_{1,1} + h_{1,2}e^{j\phi_1} + h_{2,1}e^{j\phi_2} + h_{2,2}e^{j\phi_3}|^2, \quad \phi_i = 2(n_i - 1)\pi/2^{N_i}, \\ & \quad i \in \{1, 2, 3\}, \quad n_i \in \{1, 2, \dots, 2^{N_i}\}\}. \end{aligned}$$

The result is referred by dashed curve in the figures and it is obtained by selecting best phasing through exhaustive search over all combinations. All results are presented assuming $N_1 = N_2 = N_3 = N$. In Table 1 we present required number feedback bits for SC, CS, and CC as a function of N . Note that for SS the number of feedback bits is always two and for OJC uses same number of bits with CC. We see from Figs. 5 and 6 that analytical results for both performance metrics fit well with the respective numerical results. We note that gap between upper and lower bounds for the performance, given as a difference between FI and SS performances, is 2.83dB for the SNR gain and 1.18dB for the fading figure, respectively.

We observe from Fig. 5 that SNR gain performance for SC, CS, and CC methods converge to 3.9, 4.49, and 5.25 dB, respectively, with only $N = 4$ and increasing N brings negligible improvement for any of the methods. We further note that the SNR gain for CC

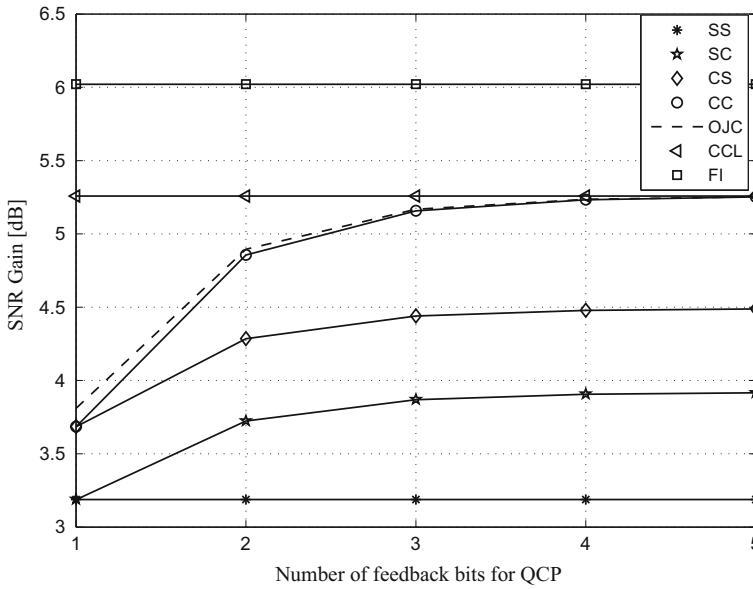


Fig. 5 SNR gain as a function of number of feedback bits used for QCP in SC, CS, and CC. *Solid curves* connect analytical results where as *markers* refer numerical results; *dashed curve* refers simulation result for OJC. Note that for SS the number of feedback bits is always two and OJC uses same number of bits with CC

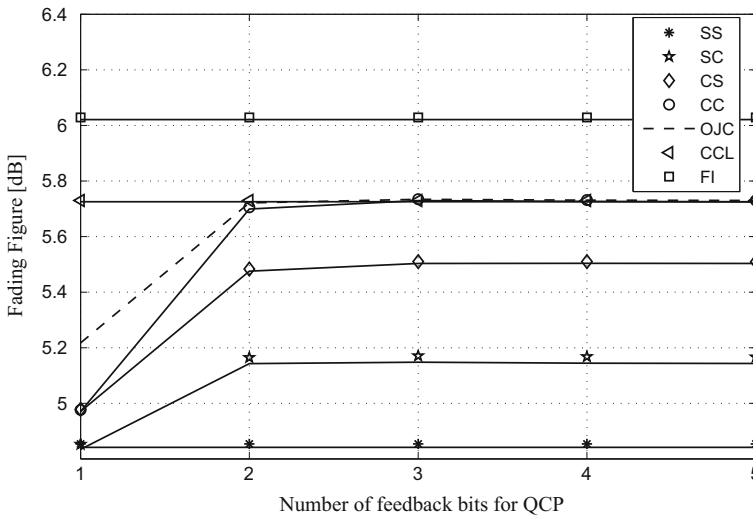


Fig. 6 Fading figure as a function of number of feedback bits used for QCP in SC, CS, and CC. *Solid curves* connect analytical results where as *markers* refer to numerical results; *dashed curve* refers simulation result for OJC. Note that for SS the number of feedback bits is always two and OJC uses same number of bits with CC

Table 1 Total numbers of required feedback bits

	$N = 1$	$N = 2$	$N = 3$	$N = 4$
SC	2	3	4	5
CS	3	4	5	6
CC	3	6	9	12

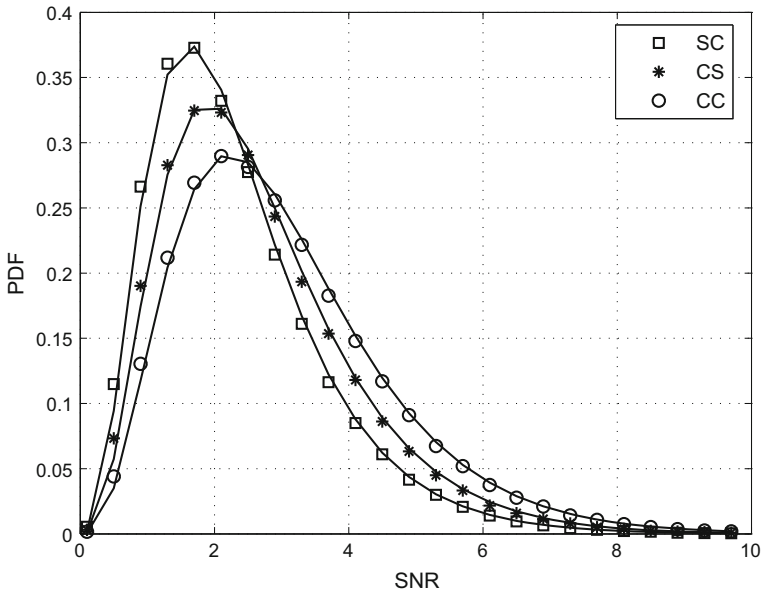


Fig. 7 Distribution of instantaneous SNR Z when SC, CS, and CC methods are applied for transmission while $N = 2$. *Solid curves* refer to approximations while as *markers* refer to numerical results

converges to $\mathcal{G}_{\text{ccl}} = (4 + 3\pi)/4$ and the largest improvement for all methods occur when N increases from 1 to 2. Furthermore, SC performs equally with SS and CC performs equally with CS when $N = 1$; otherwise, the methods perform in an increasing order of SS, SC, CS, and CC. For instance, when $N = 2$, CC, CS, and SC provide 46.85, 28.74, and 13.15% improvement relative to SS while they require 4, 2, and 1 more feedback bits (see Table 1), respectively. Moreover, CC shows negligible loss compared to the OJC for $N \geq 2$ while both methods require same number of feedback bits.

For fading figure, we see the same trend and performance order as for SNR gain, see Fig. 6. We also find that when $N = 2$, for instance, CC, CS, and SC outperform SS by 0.86, 0.63, and 0.31 dB, respectively.

The accuracy of the approximated distributions used for SC, CS, and CC is illustrated in Figs. 7 and 8 when $N = 2$ and $N = 3$, respectively. Solid curves refer to approximations while markers refer to numerical results. We observe that approximations fit well with numerical results irrespective of value of N .

Average BEP results are also presented in Figs. 9 and 10 when $N = 2$ and $N = 3$, respectively. In both figures, analytical results fit well with respective numerical results. Furthermore, we see that the performance order of different methods is the same as when measured using SNR gain i.e., FI, CCL, CC, CS, SC and SS. In terms of numerical results

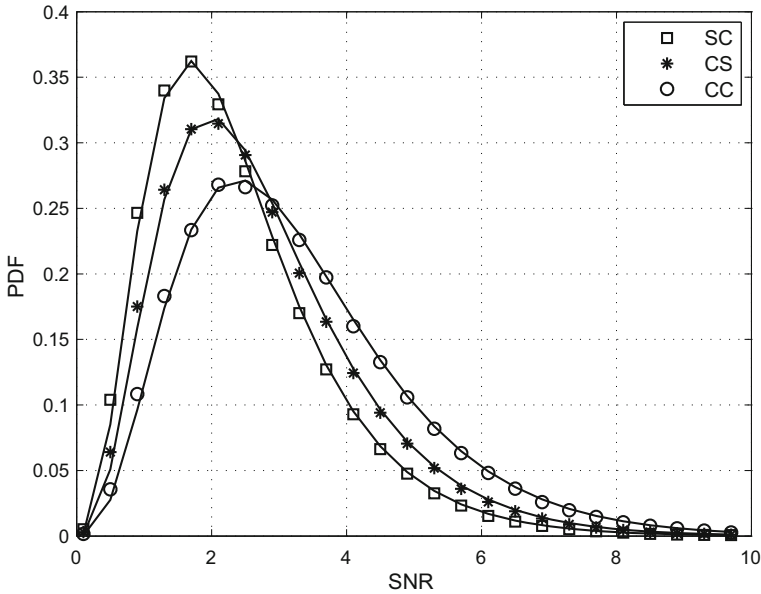


Fig. 8 Distribution of instantaneous SNR Z when SC, CS, and CC methods are applied for transmission while $N = 3$. *Solid curves* refer to approximations while *markers* refer to numerical results

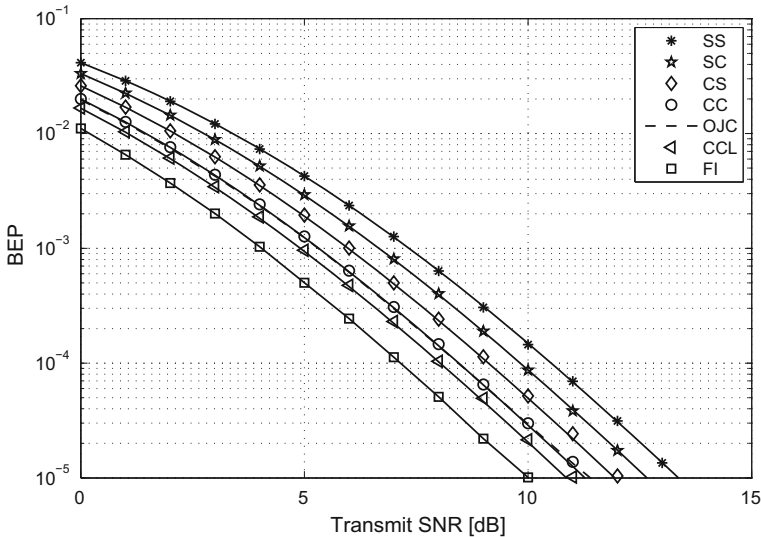


Fig. 9 Bit error probability as a function of average transmit SNR. *Solid curves* refer analytical results where as *markers* refer numerical results; *dashed curve* refers simulation result for OJC

we have with $N = 2$, a 2.5, 2.1, 1.4, and 0.7 dB SNR difference for CCL, CC, CS, and SC relative to SS at 10^{-3} average BEP value, respectively. We recall here that the CC, CS and SC require 4, 2 and 1 more feedback bits than SS as shown in Table 1. Furthermore, we

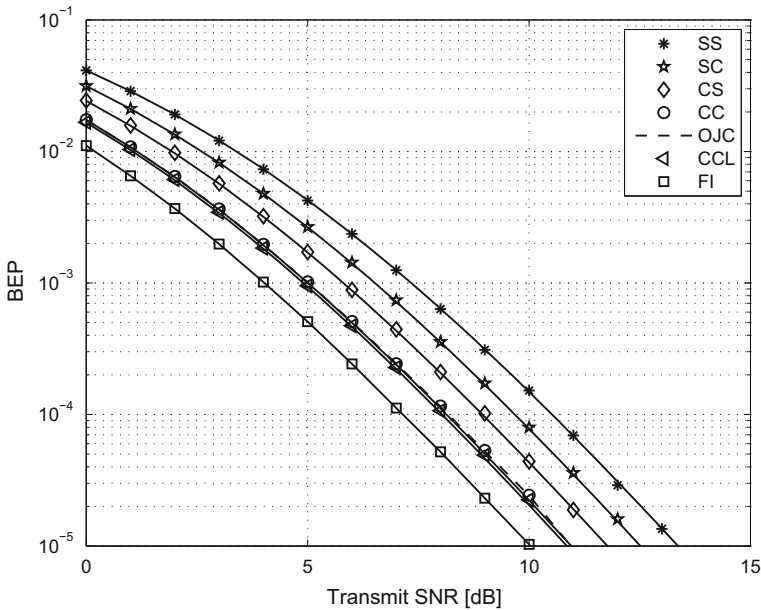


Fig. 10 Bit error probability as a function of average transmit SNR. *Solid curves* refer analytical results where as *markers* refer numerical results; *dashed curve* refers simulation result for OJC

observe that CC curve in both figures overlaps with the non-hierarchical OJC showing negligible performance difference. With $N \geq 3$, results of both converge to result of CCL which is equivalent with the non-hierarchical perfect co-phasing method.

8 Conclusion

We introduced and analyzed the performance of beamforming in presence of limited feedback with hierarchical structure. This approach can be applied when system is composed by co-located and/or distributed groups of antennas. The proposed feedback structure allows flexible implementation of combinations of different beamforming schemes with various feedback, backhaul, and other implementation requirements. For simplicity analysis was carried out for a 2×2 transmit antenna system when combining the two simple and practical beamforming methods: QCP and transmit antenna selection. For the combined methods, we derived closed-form expressions for the SNR gain, fading figure and average BEP. Performance of combined methods naturally position in between performance of the conventional antenna selection (lower performance bound) and the case where transmitter employ full CSI. Performance increase in terms of SNR gain and fading figure saturate soon when number of feedback bits is increased in QCP: SNR gain increase stop when 4 bit feedback is applied and fading figure admit almost maximum with just 3 feedback bits. Moreover, average BEP results for CC method overlap with CCL results when using only 3 feedback bits in QCP. The hierarchical CC also shows negligible performance loss compared to the non-hierarchical OJC while the former provides better implementation flexibility and sensitivity to feedback errors. Results clearly point out that

good beamforming performance can be reached with suboptimal methods that provide implementation flexibility and increased robustness against non-idealities between antenna groups. In future work, analysis will be generalized to $M \times N$ antenna structure following the approach used in this paper and employing performance measures such as outage and average capacity.

Acknowledgments This work was prepared in two projects: (1) EIT ICT LAB 'Forward Green 5G Mobile Networks' (5GrEEn) (2) Energy Efficient Wireless Networks and Connectivity of Devices-Systems (EWINE-S).

Open Access This article is distributed under the terms of the Creative Commons Attribution 4.0 International License (<http://creativecommons.org/licenses/by/4.0/>), which permits unrestricted use, distribution, and reproduction in any medium, provided you give appropriate credit to the original author(s) and the source, provide a link to the Creative Commons license, and indicate if changes were made.

Appendix 1: Error-Corrected Chi-Square Approximation

The generic distribution of Z , $f_Z(z)$, without usable and exact closed-form formula is approximated by a chi-square distribution with n degrees of freedom and mean $E[Z]$. This approximation bases on the fact that Z is chi-square random variable when there is full and perfect channel state information at the transmitter. Given the approximation is in use, the error becomes

$$\varepsilon(z) = f_Z(z) - \frac{m}{\alpha!} (mz)^\alpha e^{-mz}, \quad (36)$$

where $\alpha = n/2 - 1$ and $m = n/(2E[Z])$. The error is expressed in series form in terms of moments of Z and the generalized Laguerre polynomials (see equation (8.970, 1) in [35]) so that the corrected chi-square distribution for $f_Z(r)$ formulated as [37]

$$\begin{aligned} f_Z(z) &= \frac{m}{\alpha!} (mz)^\alpha e^{-mz} + \varepsilon(r) \\ &= \frac{m}{\alpha!} (mz)^\alpha e^{-mz} \left(1 + \sum_{k=2}^{\infty} C_k^{(\alpha)} L_k^{(\alpha)}(mz) \right), \end{aligned} \quad (37)$$

where the coefficients $C_k^{(\alpha)}$ are function of moments of Z . The orthogonality property of $L_k^{(\alpha)}(\cdot)$ is used to express these coefficients as function of the moments (see Appendix A in [37]). The series starts from $k = 2$ since the moments of the error for order up to 1 are null. When only the first term in equation (38) is considered, we find first-order corrected chi-square approximation for $f_Z(z)$. It is given by

$$\begin{aligned} f_Z(z) &\approx \frac{m}{\alpha!} (mz)^\alpha e^{-mz} \left(1 + C_2^{(\alpha)} L_2^{(\alpha)}(mz) \right) \\ &\approx \frac{m^{\alpha+1}}{\alpha!} e^{-mz} \sum_{i=1}^3 a_i z^{i+\alpha-1}, \end{aligned} \quad (38)$$

where $a_3 = 2m^2 \left[\frac{m^2 E[Z^2]}{4(\alpha+1)(\alpha+2)} - \frac{1}{4} \right]$, $a_2 = \frac{-2(\alpha+2)}{m} a_3$, and $a_1 = \frac{-E[Z]}{2} a_2 + 1$. Refer Appendix A in [37] to understand how $C_k^{(\alpha)}$, and then a_3 , a_2 and a_1 are formulated as functions of moments of Z .

Appendix 2: SNR Odd Moments for CC

For odd m , the m th moment for $|z_i|$ can be expressed as

$$\begin{aligned}
 E[|z_i|^m] &= E\left[\left(\gamma_{i,1} + \gamma_{i,2} + 2\sqrt{\gamma_{i,1}\gamma_{i,2}} \cos \theta_i\right)^{m/2}\right] \\
 &= \int_0^\infty \int_0^\infty \int_{\frac{-\pi}{2N_i}}^{\frac{\pi}{2N_i}} \frac{2^{N_i-1}}{\pi} e^{-(\gamma_{i,1}+\gamma_{i,2})} \\
 &\quad \left(\gamma_{i,1} + \gamma_{i,2} + 2\sqrt{\gamma_{i,1}\gamma_{i,2}} \cos \theta_i\right)^{m/2} d\theta_i d\gamma_{i,1} d\gamma_{i,2}.
 \end{aligned}
 \tag{39}$$

After substituting $\gamma_{i,1} = \gamma$ and $\gamma_{i,2} = t\gamma$, the integration in equation (39) becomes

$$\begin{aligned}
 E[|z_i|^m] &= \frac{2^{N_i}}{\pi} \int_0^\infty \int_0^\infty \int_{\frac{-\pi}{2N_i}}^{\frac{\pi}{2N_i}} (1 + t + 2\sqrt{t} \cos \theta_i)^{m/2} \\
 &\quad * \left[\int_0^\infty \gamma^{m/2+1} e^{-\gamma(1+t)} d\gamma \right] d\theta_i dt.
 \end{aligned}
 \tag{40}$$

Using equation (3.381, 4) in [35], the inner most integral is computed as

$$\int_0^\infty \gamma^{m/2+1} e^{-\gamma(1+t)} d\gamma = \Gamma\left(\frac{m}{2} + 2\right) \left(\frac{1}{1+t}\right)^{m/2+2}.
 \tag{41}$$

Thus, equation (40) attains the form

$$\begin{aligned}
 E[|z_i|^m] &= \frac{2^{N_i} \Gamma(m/2 + 2)}{\pi} \int_0^\infty \int_0^{\frac{\pi}{2N_i}} \frac{1}{(1+t)^2} \\
 &\quad * \left(1 + 2\frac{\sqrt{t}}{1+t} \cos \theta_i\right)^{m/2} d\theta_i dt
 \end{aligned}
 \tag{42}$$

Since $-1 < 2\frac{\sqrt{t}}{1+t} \cos \theta_i < 1$ for all ranges of t and θ_i , we can use the expansion

$$\left(1 + \frac{2\sqrt{t}}{1+t} \cos \theta_i\right)^{\frac{m}{2}} = \sum_{k=0}^\infty \frac{(-2)^k \Gamma(-m/2 + k)}{k! \Gamma(-m/2)} \left(\frac{\sqrt{t}}{1+t}\right)^k \cos^k \theta_i.
 \tag{43}$$

Therefore, equation (42) can be written as

$$\begin{aligned}
 E[|z_i|^m] &= \frac{2^{N_i} \Gamma(m/2 + 2)}{\pi} \sum_{k=0}^\infty \frac{(-2)^k \Gamma(-m/2 + k)}{k! \Gamma(-m/2)} \\
 &\quad \int_0^\infty \frac{t^{\frac{k}{2}}}{(1+t)^{k+2}} dt \int_0^{\frac{\pi}{2N_i}} \cos^k \theta_i d\theta_i.
 \end{aligned}
 \tag{44}$$

Finally, equation (42) is reduced into

$$\begin{aligned}
 E[|z_i|^m] &= \frac{2^{N_i} \Gamma(m/2 + 2)}{\pi} \\
 &\quad * \sum_{k=0}^\infty \frac{(-2)^k \Gamma(-m/2 + k)}{k! \Gamma(-m/2)} B\left(\frac{k}{2} + 1, \frac{k}{2} + 1\right) I_{N_i}(k),
 \end{aligned}
 \tag{45}$$

where $B(\cdot, \cdot)$ is the beta function as defined in [38, (6.2.1)] and $I_{N_i}(k)$ is given by

$$I_{N_i}(k) = \int_0^{\frac{\pi}{2N_i}} \cos^k \theta_i d\theta_i$$

$$= \begin{cases} \frac{\pi}{2^{2N_i+N_i}} \binom{2n}{n} + \frac{1}{2^{2n-1}} \sum_{l=0}^{n-1} \binom{2n}{l} \frac{\sin(2n-2l) \frac{\pi}{2N_i}}{2n-2l}, & k = 2n, \\ \frac{1}{2^{2n}} \sum_{l=0}^n \binom{2n+1}{l} \frac{\sin(2n-2l+1) \frac{\pi}{2N_i}}{2n-2l+1}, & k = 2n+1, \end{cases} \quad (46)$$

as defined in [35, (2.513,3,4)].

References

1. Love, D., Heath, R., Lau, V., Gesbert, D., Rao, B., & Andrews, M. (2008). An overview of limited feedback in wireless communication systems. *IEEE Journal on Selected Areas in Communications*, 26, 1341–1365.
2. Jindal, N. (2006). MIMO broadcast channels with finite-rate feedback. *IEEE Transactions on Information Theory*, 52, 5045–5060.
3. Choi, J., Kim, S. R., & Choi, I.-K. (2007). Statistical eigen-beamforming with selection diversity for spatially correlated OFDM downlink. *IEEE Transactions on Vehicular Technology*, 56, 2931–2940.
4. Pitaval, R.-A., Maattanen, H.-L., Schober, K., Tirkkonen, O., & Wichman, R. (2011). Beamforming codebooks for two transmit antenna systems based on optimum Grassmannian packings. *IEEE Transactions on Information Theory*, 57(10), 6591–6602.
5. Tao, X., Xu, X., & Cui, Q. (2012). An overview of cooperative communications. *IEEE Communications Magazine*, 50, 65–71.
6. Karakayali, M. K., Foschini, G. J., & Valenzuela, R. A. (2006). Network coordination for spectrally efficient communications in cellular systems. *IEEE Wireless Communications Magazine*, 13, 56–61.
7. Dahrouj, H., & Yu, W. (2010). Coordinated beamforming for the multicell multi-antenna wireless system. *IEEE Transactions on Wireless Communications*, 9, 1748–1759.
8. 3GPP. (2011). *Physical layer procedures (FDD)*. TS 25.214, Version 10.4.0, 3GPP Technical specification.
9. 3GPP. (2011). *Physical channels and modulation*. TS 36.211, Version 10.3.0, 3GPP Technical Specification.
10. Hottinen, A., Tirkkonen, O., & Wichman, R. (2003). *Multi-antenna transceiver techniques for 3G and beyond*. London: Wiley.
11. Hämäläinen, J., Wichman, R. (2000). Closed-loop transmit diversity for FDD WCDMA systems. In: *Proceedings of asilomar conference on signals, systems and computers*, Vol. 1, pp. 111–115.
12. Hämäläinen, J., Wichman, R., Dowhuszko, A. A., Corral-Briones, G. (2009). Capacity of generalized UTRA FDD closed-loop transmit diversity modes. *Wireless Personal Communications*, 54(3), 467–484.
13. 3GPP. (2011). *Coordinated multi-point operation for LTE physical layer aspects*. TR 36.819, version 11.0.0, 3GPP Technical Report.
14. Sun, S., Gao, Q., Peng, Y., Wang, Y., & Song, L. (2013). Interference management through CoMP in 3GPP LTE-advanced networks. *IEEE Transaction on Wireless Communications*, 20(1), 59–66.
15. Irmer, R., Droste, H., Marsch, P., Grieger, M., Thiele, G., Jungnickel, V. (2011). Coordinated multi-point: Concepts, performance, and field trial results. *IEEE Communications Magazine*, 49(2), 102–111.
16. Lee, J., Kim, Y., Lee, H., Ng, B. L., Mazzaresse, D., Liu, J., et al. (2012). Coordinated multipoint transmission and reception in LTE-advanced systems. *IEEE Communications Magazine*, 50, 44–50.
17. Sawahashi, M., Kishiyama, Y., Morimoto, A., Nishikawa, D., & Tanno, M. (2010). Coordinated multipoint transmission/reception techniques for LTE-advanced. *IEEE Wireless Communications Magazine*, 17, 26–34.
18. Love, D. J., Heath, R. W., Jr, & Strohmer, T. (2003). Grassmannian beamforming for multiple-input multiple-output wireless systems. *IEEE Transactions on Information Theory*, 49, 2735–2747.
19. Mukkavilli, K. K., Sabharwal, A., Erkip, E., & Aazhang, B. (2003). On beamforming with finite rate feedback in multiple-antenna systems. *IEEE Transactions on Information Theory*, 49, 2562–2579.

20. Hämäläinen, J., Wichman, R. L. (2002) Performance analysis of closed-loop transmit diversity in the presence of feedback errors. In: *Proceedings of IEEE international symposium on personal, indoor and mobile radio communications*, Vol. 5, pp. 2297–2301.
21. Duarte, M., Sabharwal, A., Dick, C., & Rao, R. (2010). Beamforming in MISO systems: Empirical results and EVM-based analysis. *IEEE Transactions on Wireless Communications*, 9, 3214–3225.
22. Heidari, A., & Khandani, A. (2010). Closed-loop transmit diversity with imperfect feedback. *IEEE Transactions on Wireless Communications*, 9, 2737–2741.
23. Jaramillo-Ramirez, D., Kountouris, M., Hardouin, E. (2012). Coordinated multi-point transmission with quantized and delayed feedback. In: *Proceedings of IEEE global telecommunications conference*, pp. 2391–2396.
24. Liang, L., Xu, W., Zhang, H. (2012). Adaptive coordinated multi-point transmission based on delayed limited feedback. In: *Proceedings of IEEE international symposium on personal, indoor and mobile radio communications*, pp. 2335–2340.
25. 3GPP. (2013). *Coordinated multi-point operation for LTE with non-ideal backhaul*. TR 36.874, Ver. 2.0.0, 3GPP Technical Report.
26. Zhao, J., Quek, T., & Lei, Z. (2013). Coordinated multipoint transmission with limited backhaul data transfer. *IEEE Transactions on Wireless Communications*, 12, 2762–2775.
27. Hamalainen, J., Wichman, R. (2003). On correlations between dual-polarized base station antennas. In: *Global telecommunications conference, 2003. GLOBECOM '03*. IEEE, Vol. 3, pp. 1664–1668.
28. Pedersen, K., Mogensen, P., Fleury, B. (1998). Spatial channel characteristics in outdoor environments and their impact on bs antenna system performance. In: *Vehicular technology conference, 1998. VTC 98*. 48th IEEE, Vol. 2, pp. 719–723.
29. Vaughan, R. (1990). Polarization diversity in mobile communications. *IEEE Transactions on Vehicular Technology*, 39, 177–186.
30. Turkmani, A., Arowojolu, A., Jefford, P., & Kellett, C. (1995). An experimental evaluation of the performance of two-branch space and polarization diversity schemes at 1800 mhz. *IEEE Transactions on Vehicular Technology*, 44, 318–326.
31. Lindmark, B., & Nilsson, M. (2001). On the available diversity gain from different dual-polarized antennas. *IEEE Journal on Selected Areas in Communications*, 19, 287–294.
32. Nakagami, M. (1960). The m -distribution—A general formula for intensity distribution of rapid fading. In W. C. Hoffman (Ed.), *Statistical methods in radio wave propagation* (pp. 3–34). Oxford: Pergamon Press.
33. Goldsmith, A. (2005). *Wireless communications*. Cambridge: Cambridge University Press.
34. Papoulis, A. (1984). *Probability, random variables, and stochastic processes*. New York: McGraw-Hill.
35. Gradshteyn, I. S., & Ryzhik, I. M. (2007). *Table of integrals, series, and products* (7th ed.). Amsterdam: Elsevier/Academic Press.
36. Simon, M. K., & Alouini, M.-S. (2000). *Digital communication over fading channels*. London: Wiley.
37. Dowhuszko, A. A., Corral-Briones, G., Hämäläinen, J., & Wichman, R. (2009). On throughput-fairness tradeoff in virtual MIMO systems with limited feedback. *EURASIP Journal on Wireless Communications and Networking*, 2009, 1–17.
38. Abramowitz, M., & Stegun, I. A. (1964). *Handbook of mathematical functions with formulas, graphs, and mathematical tables*, ninth Dover printing, tenth GPO printing edn. New York: Dover.



Beneyam B. Haile received his B.Sc. degree in Electrical Engineering in 2007 from Bahir Dar University, Ethiopia and his M.Sc. degree in Communication Engineering in 2010 from Aalto University, Finland. Currently, he is a Doctoral candidate in Aalto University Department of Communications and Networking, Finland. His research interest includes coordinated transmission and reception techniques, heterogeneous networks, and the planning and optimization of wireless networks.



Jyri Hämäläinen is tenured Associate Professor in the Department of Communications and Networking at the Aalto University, Finland. He earned his Ph.D. degree in Applied Mathematics at the University of Oulu in 1998 and D.Sc. (Tech.) degree in Signal Processing for Communications at the Helsinki University of Technology in 2007. In addition to his post in Aalto University, Hämäläinen is docent of Engineering Mathematics in University of Oulu and has years of experience from industry (Nokia, Nokia Siemens Networks, Ericsson). His research interests include multiantenna transmission and reception techniques, scheduling, relays, small cells, and the design and analysis of wireless networks in general. He is author or a co-author of 160 scientific publications and 35 US patents or patent applications.